Supporting Information

Facile and Robust Construction of 3D-Hierarchical $NaNbO_3$-Nanorod/$ZnIn_2S_4$ Heterojunction toward Ultra-high Photocatalytic H_2 Production

Juhua Zhang, Huajun Gu, Xinglin Wang, Huihui Zhang, Lingfeng Li, Xiaohao Wang, Wei-Lin Dai*

Department of Chemistry and Shanghai Key Laboratory of Molecular Catalysis and Innovative Materials, Fudan University, Shanghai 200433, P. R. China

1. Materials

Niobium pentaoxide (Nb_2O_5), zinc chloride ($ZnCl_2$), indium chloride tetrahydrate ($InCl_3 \cdot 4H_2O$) and thioacetamide (TAA) were purchased from Aladdin Bio-Chem Technology Co., Ltd., Sodium hydroxide (NaOH), sodium sulfide nonahydrate ($Na_2S \cdot 9H_2O$), sodium sulfite (Na_2SO_3), N, N-dimethylformamide (DMF) and glycerol were purchased from Sinopharm Chemical Reagent Co., Ltd. Deionized water and ethanol were used as received without further purification.

2. Materials characterization

The morphologies and microstructures of composites were studied using a scanning electron microscopy (SEM, Phenom Prox, Netherlands), a transmission electron microscope (TEM, JEM-2011, JOEL) and a field emission transmission

electron microscope (FE-TEM, Tecnai G2 F20 S-Twin) operated at an accelerating voltage of 200 kV. A D2 phase X-ray diffractometer (XRD, D2 PHASER) was used to measure the crystal structures of samples. X-ray photoelectron spectroscopy (XPS) measurements were performed with a RBD 147 upgraded Perkin Elmer PHI 5000C ESCA system using Mg Ka radiation and all binding energies were referenced to the contaminant carbon C 1s peak (284.6 eV) for calibration. The specific surface area (S_{BET}) was estimated at liquid nitrogen temperature (77 K) on Micromeritics Tristar 3020 by nitrogen adsorption and desorption. The UV-vis diffuse reflectance spectra (DRS) were carried on a SHIMADZU UV-2450 spectrophotometer with a wavelength range of 320-820 nm and $BaSO_4$ was used as a reflectance standard. Infrared spectra are implemented by a Fourier transform infrared spectrometer (FT-IR, Nicolet iS 10).The transfer and separation of electron−hole pairs were confirmed by photoluminescence (PL) spectra on a JASCO FP-6500 fluorescence spectrophotometer at the emission wavelength of 385 nm.

3. Calculation of AQE

The apparent quantum efficiency (AQE) of photocatalytic hydrogen evolution was measured using typical experimental setup by applying different monochromatic light filter (320, 350, 400, 420, 450 nm). 0.02 g of the as-prepared photocatalysts were dispersed under constant stirring in a 100 mL mixed solution of 10 vol% triethanolamine. The solution was irradiated with 300 W Xe for 4 h. The average intensity of irradiation is determined by a CEL-NP2000 optical power metre. Hence, AQE could be estimated according to the following equation.

$$QE\% = \frac{number\ of\ reacted\ electrons}{number\ of\ incident\ photons} \times 100\% = \frac{number\ of\ evolved\ H2\ molecules \times 2}{number\ of\ incident\ photons} \times 100\% = \frac{2 \times n_{H_2} \times N_A \times h \times c}{S \times P \times t \times \lambda} \times 100\%$$

Where n_{H2} was the amount of H_2 molecules, N_A was Avogadro constant, h was the Planck constant, c was the speed of light, S was the irradiation area, P was the intensity of irradiation light, t was the photoreaction time, and λ represented the wavelength of monochromatic light.

4. Photoelectrochemical measurements

The photocurrent response measurements, electrochemical impedance spectroscopy (EIS) and Mott-Schottky plots were performed on an electrochemical workstation (Chenhua CHI760E, China) in a conventional three electrode with a platinum plate as the counter electrode, a saturated calomel electrode (SCE) as the reference electrode and the prepared photoelectrode as the working electrode. The working electrodes were prepared by drop-coating homogeneous catalyst suspensions directly onto the F-doped SnO_2-coated glass (FTO glass) surfaces at 100 °C (1×1 cm^2) for 4 h. The transient photocurrent response of the different samples was determined in a 0.5M Na_2SO_4 aqueous solution under irradiation of a 300W Xe lamp. Electrochemical impedance spectroscopy (EIS) was accomplished at an open circuit potential, with the frequency ranging from 100 kHz to 0.01 Hz, where were in a mixed solution of potassium ferricyanide (0.025 M) and muriate of potash (0.1 M). The Mott-Schottky

measurement was conducted in the potential range from -1.0 to 0.5 V (vs RHE) with a frequency of 0.1, 0.2, 0.3 and 0.5 kHz.

5. Theoretical calculation

All spin-polarization density functional theory (DFT) calculations were performed by employing the Vienna ab initio package (VASP) [1, 2] within the generalized gradient approximation (GGA) using the Perdew-Burke-Ernzerhof (PBE)[3, 4] formulation. The electron-ion interaction was described and taken into account by the projected augmented wave (PAW) potentials [4, 5] and a kinetic energy cutoff of a plane wave basis was set with 400 eV. Partial occupancies of the Kohn-Sham orbitals were allowed using the Gaussian smearing method and a width of 0.05 eV. The electronic energy was considered self-consistent when the energy change was smaller than 10^{-6} eV. A geometry optimization was considered convergent when the energy change was smaller than 0.05 eV $Å^{-1}$. Finally, adsorption binding energies (E_b) were calculated as:

$$E_b = E_{ad/sub} - E_{ad} - E_{sub},$$

where $E_{ad/sub}$, E_{ad}, and E_{sub} were the total energies of the optimized adsorbate/substrate system, the adsorbate in the gas phase, and the clean substrate, respectively.

The free energy ΔG of the reaction was calculated as the difference between the free energies of the initial and final states using the equation:

$$\Delta G = \Delta E + \Delta ZPE - T\Delta S$$

Where *G*, *E, ZPE* and *TS* were the free energy, total energy from DFT calculations, zero point energy and entropic contributions, respectively.

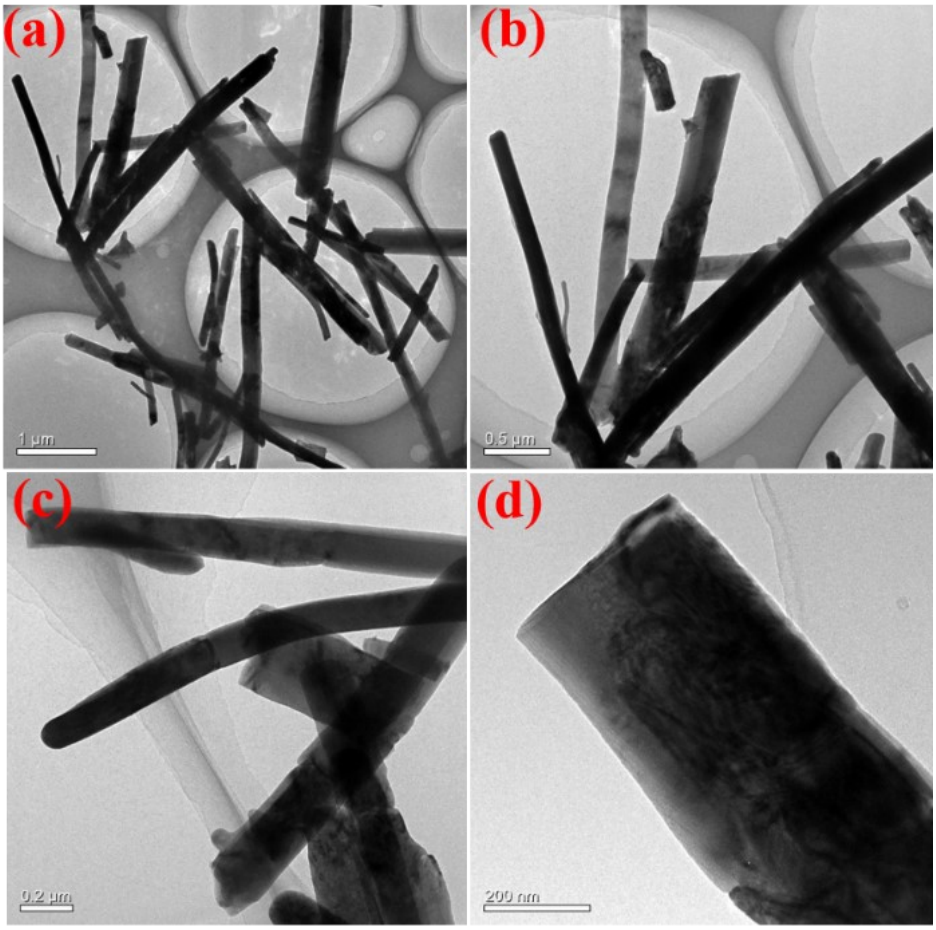

Fig. S1. TEM (a-b) and enlarged TEM images (c-d) of $NaNbO_3$ nanorods.

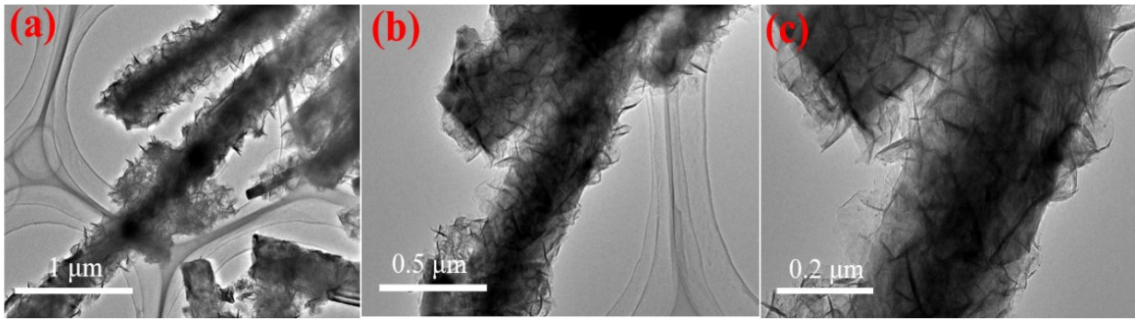

Fig. S2. TEM images of $NaNbO_3/ZnIn_2S_4$ composites.

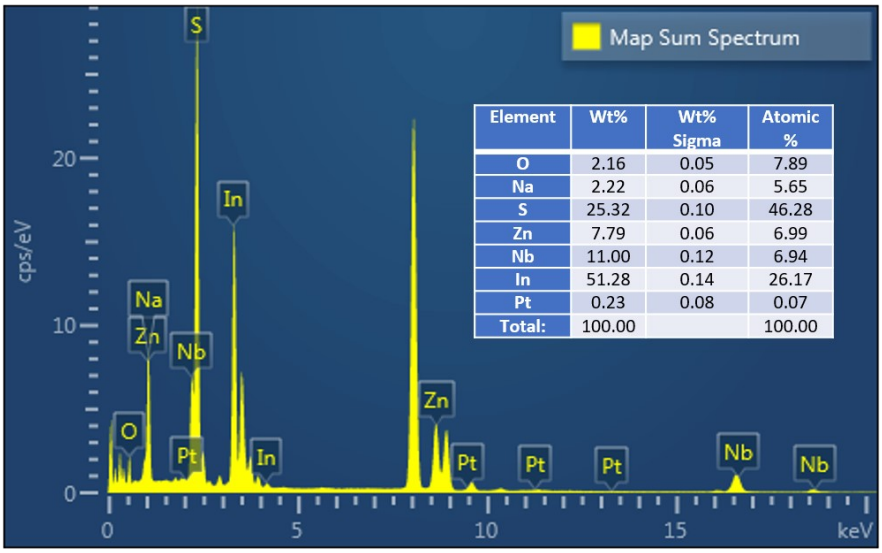

Element	Wt%	Wt% Sigma	Atomic %
O	2.16	0.05	7.89
Na	2.22	0.06	5.65
S	25.32	0.10	46.28
Zn	7.79	0.06	6.99
Nb	11.00	0.12	6.94
In	51.28	0.14	26.17
Pt	0.23	0.08	0.07
Total:	100.00		100.00

Fig. S3. EDX spectrum of $NaNbO_3/ZnIn_2S_4$ composites and inserted atomic percentages of the elements.

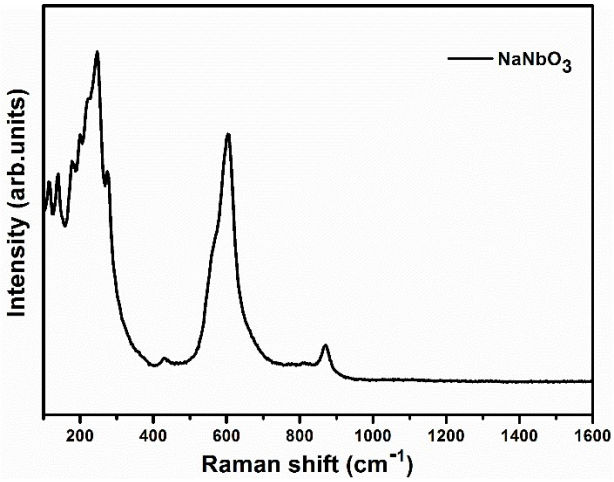

Fig. S4. Raman spectroscopy of $NaNbO_3$.

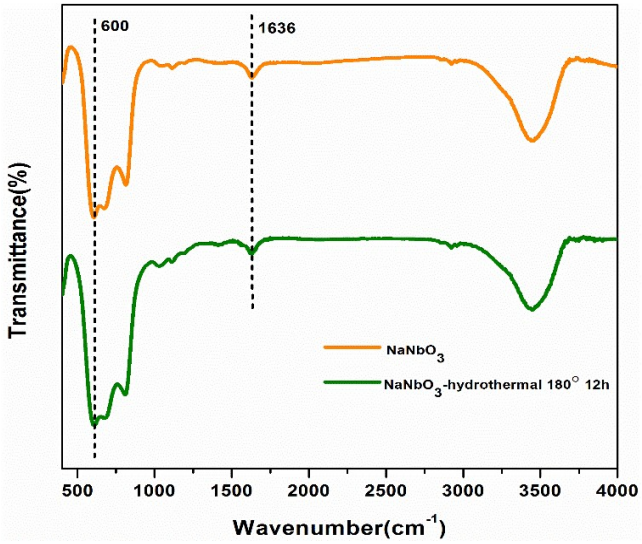

Fig. S5. FT-IR spectra of $NaNbO_3$ and $NaNbO_3$ treated with hydrothermal 180° 12h.

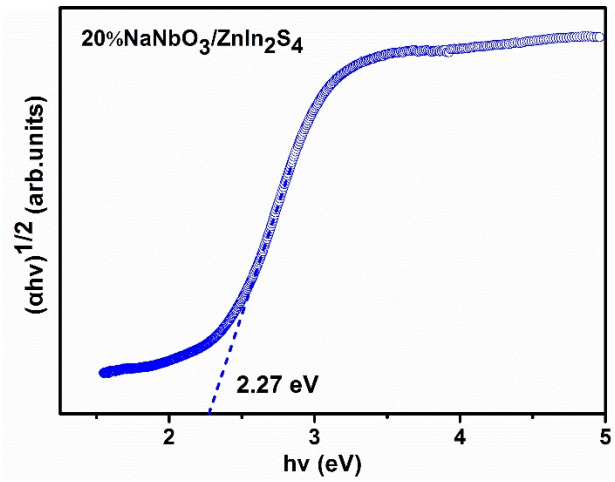

Fig. S6. Tauc plots of 20%$NaNbO_3$/$ZnIn_2S_4$.

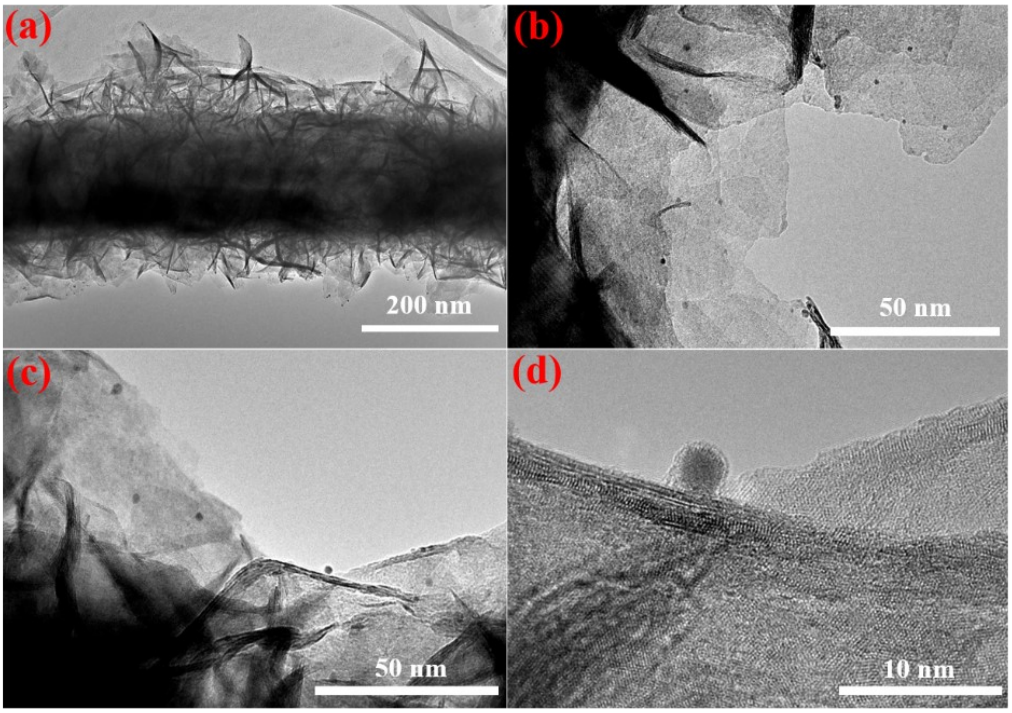

Fig. S7. TEM images (a-d) of synthesized catalysts after five cycle experiments.

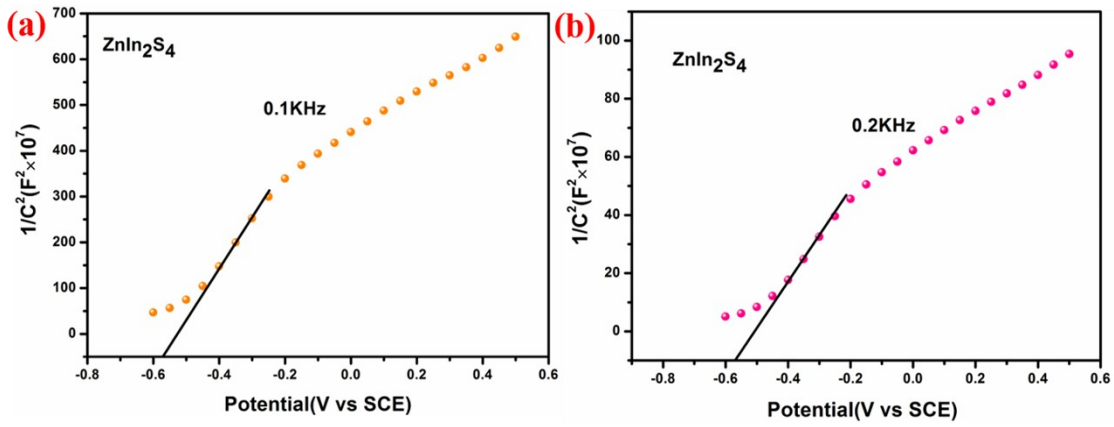

Fig. S8. Mott-Schottky plots of $ZnIn_2S_4$ under the frequency of (a) 0.1 and (b) 0.2 kHz,

respectively.

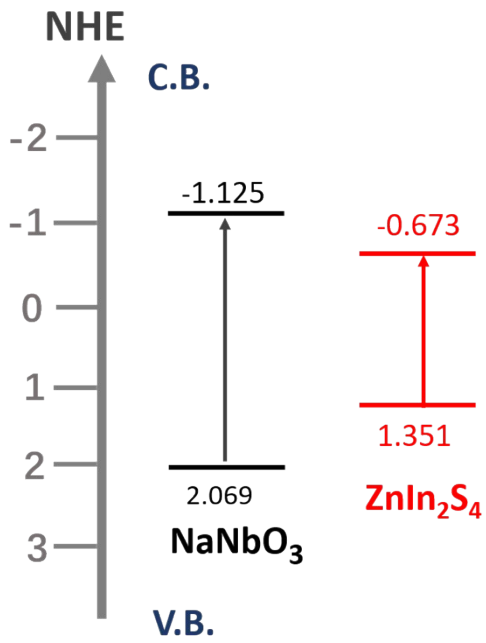

Fig. S9. The valence band maximum (VBM) and conduction band minimum (CBM) of $NaNbO_3$ and $ZnIn_2S_4$ calculated based on density functional theory.

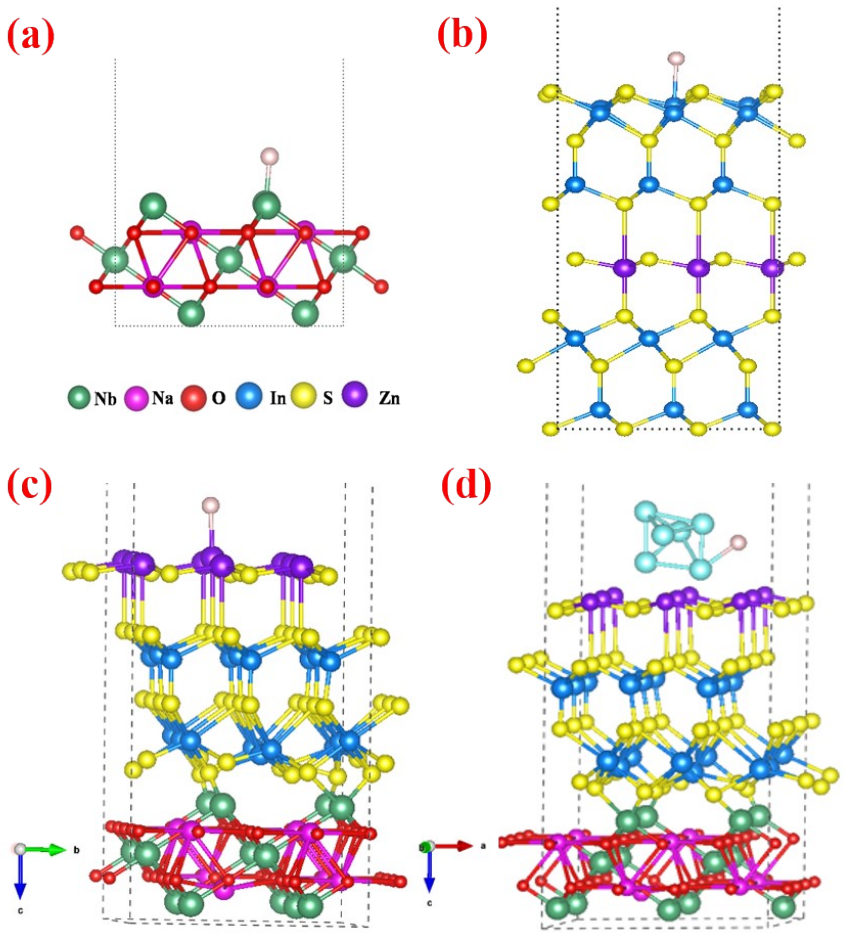

Fig. S10. atomic structures of hydrogen adsorption sites on (a) $NaNbO_3$, (b) $ZnIn_2S_4$, (c) $NaNbO_3/ZnIn_2S_4$ and (d) Pt-$NaNbO_3/ZnIn_2S_4$.

Table S1. The surface area and pore size of different samples.

Photocatalysts	$NaNbO_3$	$ZnIn_2S_4$	10%$NaNbO_3$/ $ZnIn_2S_4$	15%$NaNbO_3$/ $ZnIn_2S_4$	20%$NaNbO_3$/ $ZnIn_2S_4$	25%$NaNbO_3$/ $ZnIn_2S_4$	30%$NaNbO_3$/ $ZnIn_2S_4$
S_{BET} (m^2g^{-1})	7.9	46.3	71.8	74.3	87.7	73.4	69.5
Pore size	8.50	10.79	11.61	12.12	12.37	12.21	13.21

Table S2. Comparison of photocatalytic hydrogen evolution performance with the reported $NaNbO_3$-based photocatalysts.

Samples	Light source	Incident light (nm)	Sacrificial agents and cocatalysts	H_2 (μmol h^{-1})	Ref.
$NaNbO_3/ZnIn_2S_4$	**300 W Xe**	**>300**	**TEOA 1wt% Pt**	**600.8**	**This work**
Au/CdS/$NaNbO_3$	Hi-Tech	AM 1.5G filter	0.1M Na_2S 0.14M Na_2SO_3	54.1	[S6]
$In_2O_3/NaNbO_3$Rods	300W Xe	>300	0.8%Pt Methanol	13	[S7]

$Pt/NaNbO_3$	300W Xe	>300	Methanol	26.6	[S8]
$(LaCo)_{0.03}(NaNb)_{0.97}O_3$	300W Xe	>420	0.5%Pt Methanol	11.9	[S9]
Cubic $NaNbO_3$nanowires	300W Xe	>300	0.5%Pt Methanol	70	[S10]
$Pt/N\text{-}rGO/N\text{-}NaNbO_3$	300W Xe	>300	Methanol	46.8	[S11]
$Pt/NaNbO_3(O_2)$	300W Xe	>300	0.5%Pt Methanol	43	[S12]
$Ag/NaNbO_3$	150 W Mercury	200-600	Formic acid	100	[S13]
$NaNbO_3/CdS/NiS_2$	300W Xe	>400	Lactic acid	117.5	[S14]
$MoSx–CdS–NaNbO_3$	300W Xe	>400	Lactic acid	59.65	[S15]
$CdS/Pt/N\text{-}NaNbO_3$	300W Xe	>420	Lactic acid	284.4	[S16]

Table S3 Comparison of photocatalytic hydrogen evolution performance with $ZnIn_2S_4$-Based reported works.

Samples	Light source	Incident light (nm)	Sacrificial agents and cocatalysts	H_2 (μmol $h^{-1}g^{-1}$)	Ref.
$NaNbO_3/ZnIn_2S_4$	**300 W Xe lamp**	**>300**	**TEOA 1wt% Pt**	**30038.3**	**This work**
in-situ hydrogenated $ZnIn_2S_4$	300 W Xe lamp	>300	0.25 M Na_2SO_3 0.35 M Na_2S	2150	[S17]
$Ag_2O/ZnIn_2S_4$	300 W Xe lamp	>300	TEOA	466.8	[S18]
$ZnIn_2S_4/NH_2$-UiO-66/MoS_2	300 W Xe lamp	>300	TEOA	5690	[S19]
$ZnIn_2S_4@SiO_2@TiO_2$	300 W Xe lamp	>300	TEOA	618.3	[S20]
$ZnIn_2S_4$-MOFL	300 W Xe lamp	>300	0.25 M Na_2SO_3 0.35 M Na_2S, 2 wt% Pt	28200	[S21]

$AgFeO_2/ZnIn_2S_4$	300 W Xe lamp	>400	0.25 M Na_2SO_3 0.35 M Na_2S	9140	[S22]
$ZnIn_2S_4$/pCN	300 W Xe lamp	>400	TEOA	8601	[S23]
N-doped $ZnIn_2S_4$	300 W Xe lamp	>400	TEOA	11086	[S24]
$Mo_2C/ZnIn_2S_4$	300 W Xe lamp	≥ 400	TEOA	22110	[S25]
$ZnIn_2S_4/MoSe_2$	300 W Xe lamp	>420	0.25 M Na_2SO_3 0.35 M Na_2S	2228	[S26]
$CuInS_2/ZnIn_2S_4$	300 W Xe lamp	>420	0.25 M Na_2SO_3 0.35 M Na_2S, 2 wt% Pt	3430.2	[S27]
WO_3@$ZnIn_2S_4$	300 W Xe lamp	>420	TEOA	3900	[S28]
$ZnIn_2S_4/MoS_2$-RGO	300 W Xe lamp	>420	Lactic acid	425.1	[S29]
$ZnIn_2S_4/Ni_{12}P_5$	300 W Xe lamp	>420	0.35 M Na_2S 0.25 M Na_2SO_3	2263	[S30]
MoS_2/Cu-$ZnIn_2S_4$	300 W Xe lamp	>420	0.1M ascorbic acid	5463	[S31]
$ZnIn_2S_4/MoS_2$/CdS	300 W Xe lamp	>420	TEOA	7570.4	[S32]
NH_2-UiO-66/$ZnIn_2S_4$	300 W Xe lamp	>420	0.35 M Na_2S 0.25 M Na_2SO_3	2199	[S33]
$ZnIn_2S_4$@Co-doped NH_2-MIL-53(Fe)	300 W Xe lamp	≥ 420	0.25 M Na_2SO_3 0.35 M Na_2S, 0.5 wt% Pt	26954.1	[S34]

Reference

1. G. Kresse and J. Furthmiiller, *Comput. Mater. Sci,* 1996, **6**, 15-50.
2. G. Kresse and J. Furthmuller, *Phys. Rev. B*, 1996, **54**, 11169-11186.
3. John P. Perdew, Kieron Burke and M. Ernzerhof, *Phy. Rev. Let,* 1996, **78**, 3865-3868.
4. G. Kresse and D. Joubert, *Phy. Rev. B*, 1999, **59**, 1758-1775.
5. P.E. Blochl, *Phys. Rev. B*, 1994, **50**, 17953-17979.

6. K. Nanda, H. Jain, S. Swain and S. Chaudhary, *SMC Bulletin*, 2018, **9**.
7. J. Lv, T. Kako, Z. Li, Z. Zou and J. Ye, *J. Phys. Chem. C*, 2010, **14**, 6157-6162.
8. Q. Liu, Y. Chai, L. Zhang, J. Ren and W. Dai, *Appl. Catal., B*, 2017, **205**, 505-513.
9. P. Li, H. Abe and J. Ye, *Int. J. Photo of Photoenergy*, 2014. 38042.
10. Q. Gu, K. Zhu, N. Zhang, Q. Sun, P. Liu, J. Liu, W. Jing and Z. Li, *J. Phys. Chem. C,* 2015, **119**, 25956-25964.
11. F. Yang, Q. Zhang, L. Zhang, M. Cao, Q. Liu and W. Dai, *Appl. Catal., B*, 2019, **257**, 117901.
12. N. Chen, G. Li and W. Zhang, *Physica B*. 2014, **447**, 12-14.
13. Z. Beata, E. Borowiak-Palen and R. Kalenczuk, *J. Phys. Chem. Solids*, 2011, **72**, 117-123.
14. J. Xu, J.Zhu, J. Niu, M. Chen and J. Yue, *Front Chem*, 2019, **7**, 880.
15. J. Zhu, J. Xu, X. Du, Q. Li, Y. Fu and M. Chen, *Dalton Trans*. 2020, **49**, 8891-8900.
16. F. Yang, Q. Zhang, J. Zhang, L. Zhang, M. Cao and W.-L. Dai, *Appl. Catal., B*, 2020, **278**, 119290.
17. Y. Zhu, L. Wang, Y. Liu, L. Shao and X. Xia, *Appl. Catal., B*, 2018, **241**, 483-490.
18. Y. Xiao, Z. Y. Peng, W. Zhang, Y. Jiang and L. Ni, *Appl. Surf. Sci*, 2019, **494**, 519-531.
19. Q. Ran, Z. Yu, R. Jiang, L. Qian, Y. Hou, F. Yang, F. Li, M. Li, Q. Sun and H. Zhang, *Catal. Sci. Technol.*, 2020, **10**, 2531-2539.
20. L. Wang, H. Zhou, H. Zhang, Y. Song, H. Zhang and X. Qian, *Inorg. Chem*, 2020, **59**, 2278-2287.
21. Q.Zhang, H. Gu, X. Wang, L. Li, J. Zhang, H. Zhang, Y. Li and W.-L. Dai, *Appl. Catal., B*, 2021, **298**, 120632.
22. D. Kong, H. Fan, D. Yin, D. Zhang, X. Pu, S. Yao and C. Su, *ACS Sustain. Chem. Eng*, 2021, **9**, 2673-2683.
23. H. Yang, R. Cao, P. Sun, J. Yin, S. Zhang and X. Xu, *Appl. Catal. B*, 2019, **256**, 117862.
24. C. Du, B. Yan, Z. Lin and G. Yang, *J. Mater. Chem. A*, 2020, **8**, 207-217.
25. C. Du, B. Yan and G. Yang, *Nano Energy*, 2020, **76**, 105031.
26. D. Zeng, L. Xiao, W.-J. Ong, P. Wu, H. Zheng, Y. Chen and D.-L. Peng, *ChemSusChem*, 2017, **10**, 4624-4631.
27. Z. Guan, J. Pan, Q. Li, G. Li and J. Yang, *ACS Sustainable Chem. Eng*, 2019, **7**, 7736-7742.
28. L. Ye and Z. Wen, *Int. J. Hydrogen Energy*, 2019, **44**, 3751-3759.
29. Z. Guan, P. Wang, Q. Li, G. Li and J. Yang, *Dalton Trans*, 2018, **47**, 6800-6807.
30. D. Zeng, Z. Lu, X. Gao, B. Wu and W. Ong, *Catal. Sci. Technol*, 2019, **9**, 4010-4016.
31. Y.-J. Yuan, D. Chen, J. Zhong, L.-X. Yang, J. Wang, M.-G. Liu, Z.-T. Yu and Z.-G. Zou, *J. Mater. Chem. A*, 2017, **5**, 15771-15779.
32. L. Wang, H. Zhou, H. Zhang, Y. Song, H. Zhang, L. Luo, Y. Yang, S. Bai, Y. Wang and S. Liu, *Nanoscale*, 2020, **12**, 13791-13800.

33. J. Jiang, Q. Zhu, Y. Guo, L. Cheng, Y. Lou and J. Chen, *B. Chem. Soc. Jpn*, 2019, **92**, 1047-1052.
34. F. Dai, Y. Wang, X. Zhou, R. Zhao, J. Han and L. Wang, *Appl. Surf. Sci*, 2020, **517**, 146161.